Lab on a Chip

Accepted Manuscript

ROYAL SOCIETY OF CHEMISTRY

www.rsc.org/loc

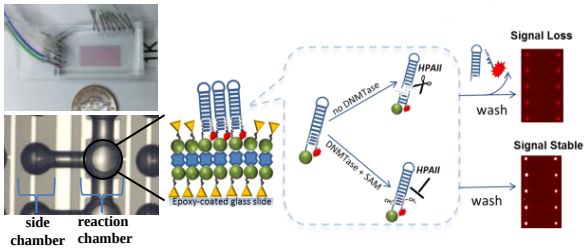

Microfluidic-based fluorometric methylation assay for functional regulation of methyltransferase activity compatible with high-throughput screening of chemical and biological libraries.

Article type: Full Paper

A Sensitive Microfluidic Platform for High Throughput DNA Methylation Assay

*Maria Ronen, Dorit Avrahami, Doron Gerber**

M. Ronen, Dr. D. Avrahami, Dr. D. Gerber
The Mina & Everard Goodman Faculty of Life Sciences, The Nanotechnology Institute
Bar-Ilan University, Ramat Gan, Israel, 5290002

E-mail: Doron.Gerber@biu.ac.il

Keywords: DNA methylation; integrated microfluidics; non-nucleoside inhibitors; high throughput screen

DNA methylation is an epigenetic modification essential for normal development and maintenance of somatic biological functions. DNA methylation provides heritable, long-term chromatin regulation and aberrant methylation pattern is associated with complex diseases including cancer. Discovering novel therapeutic targets demands development of high-throughput, sensitive and inexpensive screening platforms for libraries of chemical or biological matter involved in DNA methylation establishment and maintenance. Here, we present a universal, high-throughput, microfluidic-based fluorometric assay for studying DNA methylation *in-vitro*. The enzymatic activity of bacterial *HPAII* DNA methyltransferase and its kinetic properties are measured using the assay (K_m^{DNA}=5.8nM, K_m^{SAM}=9.8nM and K_{cat}=0.04 sec^{-1}). Using the same platform, we then demonstrate a two-step approach for high-throughput *in-vitro* identification and characterization of small molecule inhibitors of methylation. The approach is examined using known non-nucleoside inhibitors, SGI-1027 and RG108, for which we measured IC_{50} of 4.5µM and 87.5nM, respectively. The dual role of the microfluidic-based methylation assay both for the quantitative characterization of enzymatic activity and high-throughput screening of non-nucleoside inhibitors coupled with quantitative characterization of the inhibition potential, highlights the advantages of our system for epigenetic studies.

1. Introduction

DNA methylation is an epigenetic modification of DNA carried out by the DNA methyltransferase family enzymes (DNMTases), which catalyze the transfer of a methyl group from S-adenosyl methionine (SAM) to the cytosine target nucleotide producing methylcytosine (5mC).[1,2] In mammals, the methylation of cytosine nucleotide occurs predominately in the context of symmetric 5' cytosine-guanine (CpG) dinucleotides with approximately 70%-90% of all CpGs methylated in adult mammal.[3] DNA methylation is necessary for many fundamental processes, such as gene repression, parental imprinting, X-chromosome inactivation, and suppression of repetitive genomic elements, thereby making proper DNA methylation pattern essential to normal development and maintenance of somatic biological functions.[3–6] Furthermore, all cancer cells display profound disruptions in DNA methylation patterns that include extensive DNA hypomethylation, specifically at repetitive DNA elements, as well as region-specific hypermethylation at normally unmethylated regions.[7] The hypomethylation of repetitive elements contributes to genomic instability, while hypermethylation of promoters leads to silencing of genes necessary for regulating cell proliferation, apoptosis and DNA repair.

Clearly aberrant methylation patterns lead to complex diseases making proteins involved in DNA methylation establishment and maintenance important targets for the design of novel therapeutic compounds.[8] In fact, nucleoside inhibitors of DNMTase activity (DNMTIs) such as 5-aza-cytidine and 5-aza-2'-deoxycytidine have been approved by FDA for treatment of myelodysplastic syndrome. These compounds have a complex mode of action that includes cell cycle-dependent incorporation into DNA, covalent trapping of DNMTs and initiation of proteolysis and DNA damage repair machinery resulting in reactivation of tumor suppressed genes.[9] However, the nonspecific mechanism of nucleosides incorporation may cause global genomic demethylation leading to chromosomal instability.[10,11] In this relation, non-nucleoside analogues, that directly inhibit DNMTase activity, are considered a promising therapeutic target that escapes toxicity associated with DNA incorporation.[12,13] Functional regulation of DNMTase catalytic activity by

cellular protein factors could be additional strategy for less-toxic treatment of epigenetic defects. However, cellular DNMTase regulation is currently not well understood and the drug targets are limited.

Practically, discovery of novel therapeutic compounds or drug targets requires high throughput screens to cover the different chemical and biological combinations. Thus, higher experimental capacity and lower material demands are desirable. In this context, recent advances in integrated microfluidic technology have demonstrated considerable promise for effective cell biology and biomedical research.[14,15] The field of microfluidics is characterized by manipulation of working fluids at the sub-micrometer length scale.[16] Scaling laws predict that molecular assays performed in very small volumes are advantageous in terms of throughput allowing hundredfold increase in the number of assays that can be placed on a given area.[17] Consequently, microfluidic platforms provide lower consumption of reagents per reaction leading to substantial cost reduction. Additionally, scaling effects result in faster processing and response times coupled with enhanced efficiency and sensitivity[18]. Finally, high degree of parallelization and multiplex analysis add further advantages to the microfluidic approach for early stages of drug development.

While there are several known methods specific to DNA methylation dynamics research, focusing on gel electrophoresis, isotope-labeled SAM and immune reactions, each method has unnecessary drawbacks, including time-consuming treatments, the use of radioactive substances, costly antibodies and sequencing services.[19–24] Although additional non-radioactive and non-immunological methods have been developed recently, these approaches are still limited in sensitivity, generality and/or scope.[25,26] Here, we have developed an alternative method for studying DNA methylation in high throughput. This method is based on a microfluidic platform and coupled to fluorometric methylation assay that uses an endonuclease digestion approach for DNA methylation analysis. The microfluidic platform offers an advantage of performing thousands of methylation reactions in nanoliter reaction volumes on a single device within isolated reaction units. The microfluidic-based methylation assay could be subjected to high-throughput screening of large-

scale chemical/biological libraries for novel DNMTIs or cellular proteins involved in DNA methylation regulation.[27]

2. Experimental Section

Hairpin Design: DNA oligonucleotides were ordered from IDT, Belgium (5-Biotin-TTGATATGTCCGGCTCTGAGCACAGAGCCGGACATATCA-Cy5-3, Tm=67.8^{o}C).

Microfluidic Chip Design: A double-layer microfluidic device composed of a flow and a control layers is designed as described previously.[27,28] Briefly, the device consists of 64x16 reaction units array, in the flow layer, accessed through several input holes and drained into a single output (**Figure 1**a). Micromechanical ‘address‘ valves compartmentalize the microfluidic device to allow setting up to 16 separate reaction conditions on a single device within isolated columns. Each reaction unit divides into two chambers and controlled by three types of micromechanical valves: 'neck', 'button', and 'sandwich'. A side chamber that may contain dry spotted material is blocked by the 'neck' valve until exposed to reaction components. Trapping and mechanical washing of surface bound substrate in the reaction chamber is performed by the 'button' valve. The 'sandwich' valve enables each reaction to occur in its own isolated reaction unit. An average unit height is 10μm, and the average cell volume per chamber is less than 1nl.

Microfluidic Device Fabrication: The microfluidic devices were fabricated as described previously.[27,28] In short, the flow and control layers were prepared separately on silicone molds casting silicone elastomer polydimethylsiloxane (PDMS, SYLGARD 184, Dow Corning, USA). A 5:1 ratio of PDMS to curing agent was mixed for the control layer, followed by degassing, baking and access holes piercing steps. As for the flow layer, a 20:1 ratio of PDMS to curing agent was mixed, spin-coated at 2000 rpm and baked. The flow and control layers were aligned manually and the fabrication was completed by a final baking and piercing of the flow channel access holes. Finally, the two-layer chip was placed on the epoxy-coated glass slide and baked at 80^{o}C for 4 hours.

Surface Chemistry and DNA Immobilization: In order to prevent non-specific adsorption and to control for suitable binding orientation, all accessible surface area within the microfluidic device was chemically modified.[28] Biotinylated-BSA (1 μg/μl, Pierce) was flowed for 20 min through the device, binding the BSA to the epoxy surface. On top of the biotinylated-BSA, 0.5 μg/μl of Stepavidin (Neutravidin, Pierce) was added for 20 min. The 'button' valves were then closed and biotinylated-BSA was flowed through the chip again, thereby completing the surface chemistry step. For DNA immobilization, the 'button' valve was opened and biotinylated Cy5-conjugated hairpin-shaped DNA oligonucleotides (10nM, Integrated DNA Technologies) were flowed through the chip for 20 min. The biotinylated oligonucleotides immobilized to the exposed streptavidin, specifically at the area under the 'button' creating a DNA array that serves a substrate for methylation reaction. Hepes (50 mM) was used for washing un-reacted substrate between each surface chemistry step. In order to ensure the homogeneity of binding, fluorescence intensity of Cy5 was measured with a microarray scanner (LS reloaded, Tecan) using 633 nm laser and 670 nm filter. Throughout the experiments, DNA probes of different methylation states/concentrations were used. The different DNA variants were flowed one by one into separate columns within the microfluidic chip, preventing reagents from mixing. Experiment images were analyzed with GenePix7.0 (Molecular Devices).

Dynamic Range Evaluation: 10 μl of endonuclease reaction mix consisting of FastDigest *HPAII* endonuclease (1 unit, New England BioLabs) and *HPAII* 1x FastDigest buffer was prepared and flowed through the microfluidic device for 10 minutes. Then, the 'button' valve was opened to expose the immobilized DNA substrate to the enzyme and the reaction was incubated at 37^{o}C for 30 minutes. The unbound products of endonuclease activity were washed away with Hepes (50 mM) and the fluorescence intensity of Cy5 was measured as described earlier.

Polyacrylamide 10% Gel Electrophoresis: Methylation reaction products were examined by denaturing (urea) polyacrilamide 10% gel electrophoresis (Urea-PAGE) using standard protocols.

Methylation Activity of Bacterial DNMTase: For the methylation reaction, 10 µl of reaction mix containing *HPAII* DNMTase (2 units, New England BioLabs), SAM (80 µM) and 1x *HPAII* reaction buffer was prepared and the solution was loaded onto the microfluidic device for 5 minutes. After the introduction was complete, the 'sandwich' valves were closed to prevent any contamination between chambers, and the 'button' valves were opened exposing the immobilized DNA substrate to the enzymatic reaction. The microfluidic device was then incubated at 37^{o}C for 2 hours. Next, the device was washed with Hepes (50 mM) for 5 minutes, followed by loading the endonuclease reaction mix onto the microfluidic device and incubation (as described above). Finally, the cleaved DNA products were washed away and the fluorescence intensity of Cy5 was measured as described above. Throughout the experiments, DNA probes of different methylation states were used, representing positive and negative controls of the methylation assay. As mentioned previously, the methylation reaction and both controls were flowed one by one into separated columns within the microfluidic chip, preventing reagents from mixing.

HPAII DNMTase Kinetic Properties Evaluation: For the dose-dependency assay, the unmethylated DNA probe was exposed to varied concentrations of *HPAII* DNMTase (0 - 2 units) followed by endonuclease cleavage. The K_m values were determined by a kinetic analysis of the substrate-dependent product formation plots fitted by the Michaelis-Menten equation (V=Vmax(S)/Km+(S)). For K_m^{DNA} calculations, the DNA probe concentrated between 0 to 1µM was used, at constant concentration of SAM (80µM). For K_m^{SAM} calculations, SAM concentrated between 0 to 80 µM was used, at constant DNA probe concentration. For the initial velocity calculation, the methylation reaction was performed with 0.25, 0.5, 0, 1, and 2 units of *HPAII* DNMTase for 5 minutes through four independent experiments. The product fluorescent signal values were plotted against incubation time and the initial velocity was estimated from the slope of linear regression. The initial rates were linear with protein concentrations, and the K_{cat} was determined from the slope of the linear regression. Actual *HPAII* concentration was determined by its absorbance at 280nM using theoretical extinction coefficient and Bradford Protein Assay.

Small Molecules Spotting: For the inhibition array spotting, SGI-1027 and RG108 were purchased from Selleckchem and prepared in final concentrations of 1mM and 100µM, respectively. Each sample solution contained 0.125% of polyethylene glycol (CELL Associated) and 12.5 mg/ml D-Trehalose (Sigma) to prevent irreversible binding as well as for visualization during alignment. Adenosine triphosphate (ATP) and nicotinamide (NAM) were prepared in a similar way (at 10mM and 5mM, respectively) and used as negative controls of inhibition reactions. All samples were spotted onto epoxy-coated glass slides (CEL Associates) with a MicroGrid 610 microarrayer (Bio Robotics) using SMT-S75 silicone pins (Parallel Synthesis, USA). Each printed block contained 4 columns and 16 rows with a pitch of 281.25 µm by 562.5 µm, respectively. Finally, the microfluidic device was manually aligned to the spotted microarray, while ensuring the isolation of each spot within the side chamber of its own reaction unit, and bonded overnight on a heated plate at 80°C.

High-Throughput on-chip DNMTase Inhibition Assay: For the inhibition assay, a microfluidic device with aligned microarray was used. Following the surface chemistry and DNA immobilization phases, the 'button' valves were closed and the side chambers were flooded with 10µM of methylation reaction mix (2 units of *HPAII* DNMTase, 1.6 µM SAM and 2x *HPAII* reaction buffer). Then, the microfluidic chip was incubated for 30 min at room temperature allowing the spotted molecules to solubilize and react with the methylation reaction components. Next, the 'button' valves were opened, exposing the immobilized DNA substrate to the methylation reaction. The chip was, then, incubated for 2 hour at 37^{o}C. Finally, the DNA was digested with *HPAII* endonuclease and the fluorescence intensity of Cy5 was measured (as described above). For qualitative inhibition calculations, each end data set (T_{30}) was normalized to the initial fluorescence signal (T_0) within the correspondent blocks. Inhibition threshold was determined as two standard deviations below the averaged ‘unspotted’ ratio and the inhibition potential was estimated as a relative decay below the cutoff point.

IC_{50} calculations: The independent dose-dependence experiments were performed using concentration range of 1.56µM – 100µM for SGI-1027 and 6.4nM - 100µM for RG108. Each reaction with its corresponding inhibitor concentration was introduced into separated column within the microfluidic chip, preventing different concentrations from mixing. As described above, the methylation reaction components and the inhibitor were incubated together for 30 minutes, followed by exposing the DNA substrate to the methylation reaction. At the end, the DNA was digested with *HPAII* endonuclease and the fluorescence intensity of Cy5 was measured (as described earlier). IC_{50} was estimated by fitting data to three-parametric logistic curve using the formula Y=a+(b-a)/(1+10^(X-c)) (a, b and c represent minimum signal, maximum signal and $logEC_{50}$, respectively) (BioDataFit, Chang BioScience).

2. Results

2.1 *On-chip* Methylation Assay Design

The methylation assay we designed relies on a principle of methylation-dependent endonuclease digestion of DNA. The substrate DNA probe constructed of hairpin-shaped DNA oligonucleotides contains a single CpG methylation site within the recognition sequence of methylation-sensitive *HPAII* endonuclease (C↓**CG**G), a 5'-conjugated biotin moiety and 3'-conjugated Cy5 dye serving as a reporter of internal cytosine methylation status (**Figure 1**b). An initial high Cy5 signal is achieved by immobilizing DNA probes on the microfluidic device surface through biotin-avidin interactions. A methylation event should protect the DNA from cleavage, thus the fluorescence signal will remain high. If no methylation occurs, the unmethylated recognition site will be cleaved leading to the Cy5 reporter washout and fluorescent signal decrease within the corresponding chambers. A methylated version of the same DNA probe was used as a positive control of methylation event.

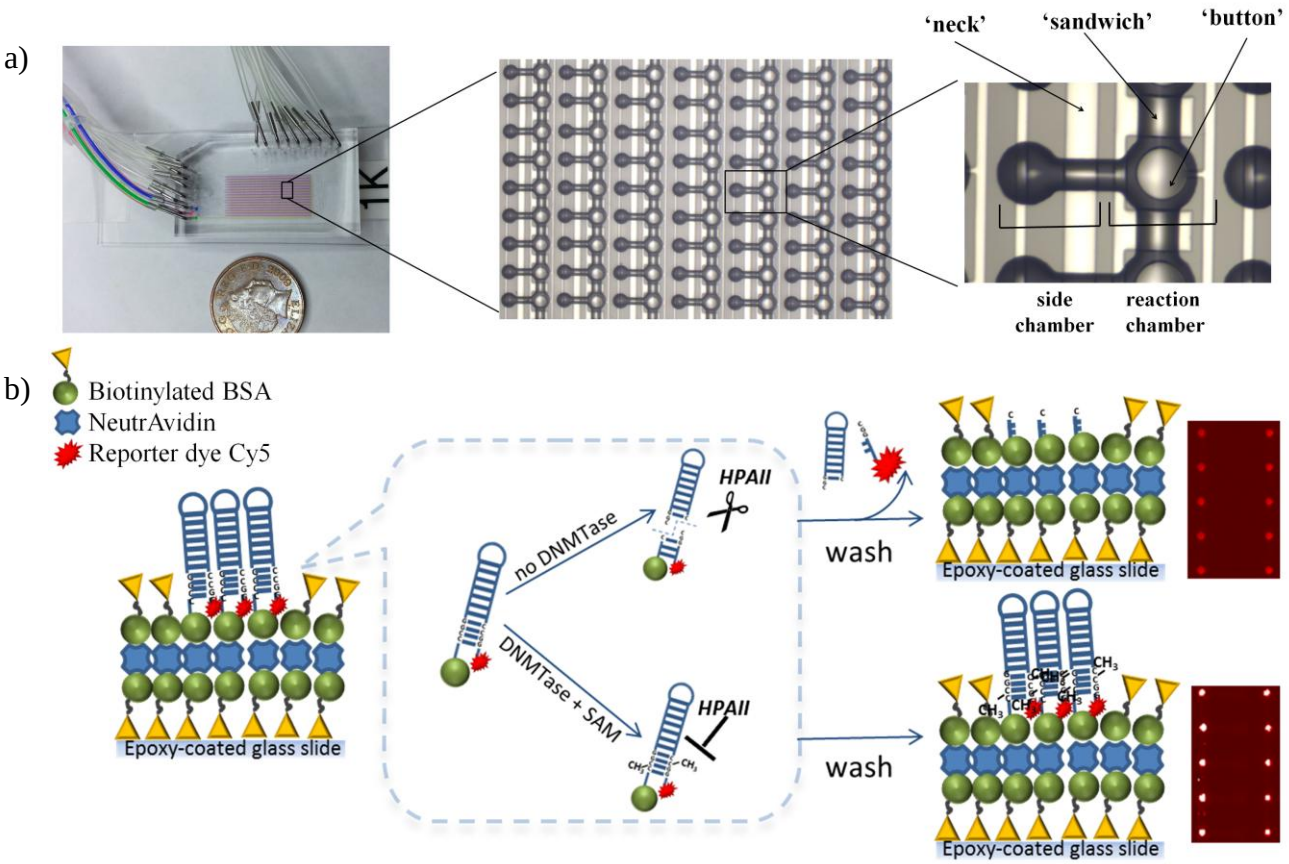

Figure 1. a) A photo and a schematic representation of the microfluidic device consisting of flow (black) and control (white) layers. The most right panel demonstrates a single reaction unit composed of two chambers and controlled by three types of micromechanical valves: 'neck', 'button', and 'sandwich'. Average cell height is 10μm, and average cell volume per unit cell is less than 1nl. b) A schematic representation of the microfluidic-based methylation assay using biotinylated hairpin-shaped DNA probe substrate. The DNA probe is immobilized to the surface through biotin-avidin interactions. Only in case of methylation event, the recognition site becomes resistant to *HPAII* activity. Otherwise, the unprotected DNA probe is digested and the unbound Cy5-containing DNA piece is washed out leading to overall fluorescent signal decrease.

2.2 Dynamic Range Evaluation

First, we evaluated the maximum dynamic range created following the *on-chip* endonuclease cleavage of methylated (protected) and unmethylated (unprotected) DNA probes. Greater range will result in higher sensitivity and reduced false-negative rate. The results showed more than 15-fold difference between the Cy5 signals of the two DNA probes (**Figure 2**a). Throughout several independent experiments, we observed constant, up to 20% signal reduction of endonuclease-resistant methylated DNA probe. This could either be attributed to bleaching, dissociation of DNA hairpins from the surface or a result of partial digestion. Denaturing Urea-PAGE separation confirmed the complete protection of methylated DNA (**Figure 2**b). Based on this, we assume that

the signal reduction originates from bleaching effect or dissociation of surface-bound DNA probes over incubation time. This decay does not affect the dynamic range significantly.

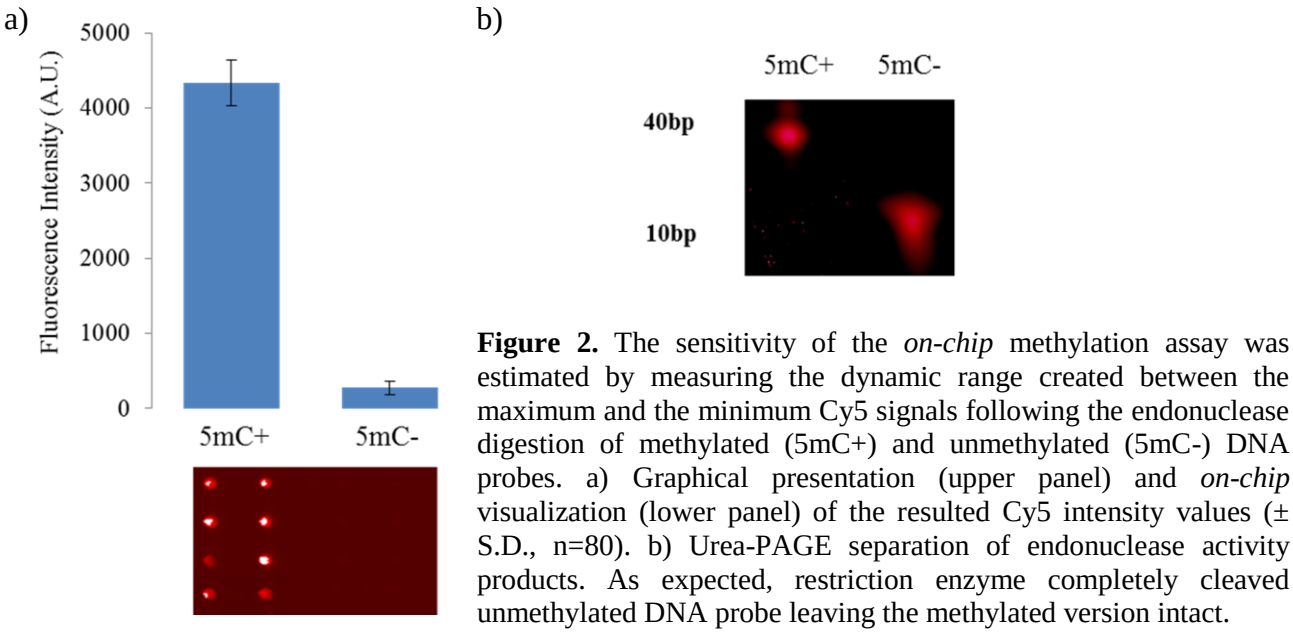

Figure 2. The sensitivity of the *on-chip* methylation assay was estimated by measuring the dynamic range created between the maximum and the minimum Cy5 signals following the endonuclease digestion of methylated (5mC+) and unmethylated (5mC-) DNA probes. a) Graphical presentation (upper panel) and *on-chip* visualization (lower panel) of the resulted Cy5 intensity values (± S.D., n=80). b) Urea-PAGE separation of endonuclease activity products. As expected, restriction enzyme completely cleaved unmethylated DNA probe leaving the methylated version intact.

2.3 Methylation Activity of Bacterial DNMTase

Next, we tested the methylation potential of the bacterial *HPAII* DNMTase (*H. parainfluenzae*). We have chosen this specific enzyme since it recognizes and methylates an internal cytosine within CCGG recognition sequences thus protecting the DNA from being accessible for digestion by methylation-sensitive *HPAII* endonuclease. According to the methylation assay design, we assumed that positive methylation event will protect the DNA probe from endonuclease cleavage and, thus, the initial fluorophore signal will be retained following the exposure to endonuclease. In agreement with this expectation, the addition of DNMTase to unmethylated DNA probe resulted in about 97% stability of the initial fluorescence signal (**Figure 3**a). The complete protection of the DNA was confirmed by denaturing Urea-PAGE separation. Based on these results, we concluded that the *on-chip* methylation reaction resulted in a digestion-protected DNA hairpin induced by *HPAII* DNMTase. We further tested the dependency of methylation product on varied concentrations of *HPAII* DNMTase. As shown in **Figure 3**b, the fitted curve formed a typical mode of saturable enzyme-catalyzed reaction, characterized by a nonlinear relationship between the response and the

amount of the enzyme. This outcome confirms the methylation activity of bacterial DNMTase achieved within microfluidic-based platform.

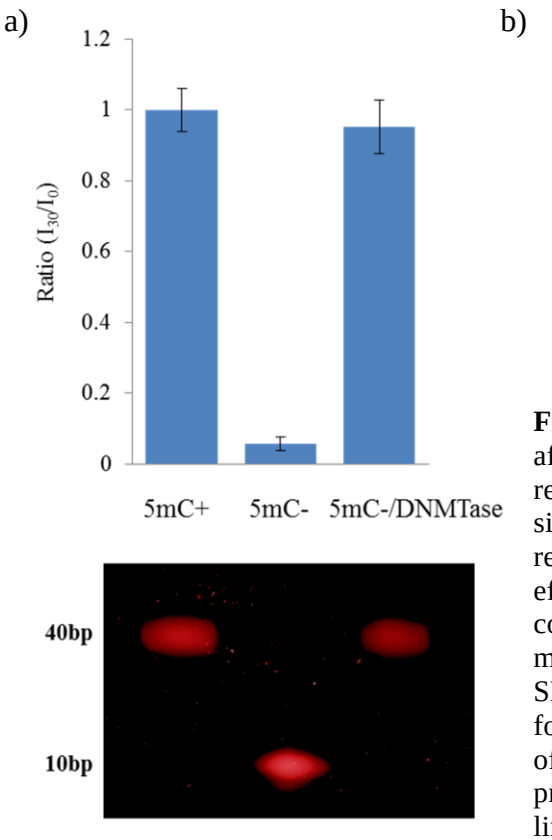

Figure 3. a) Cy5 intensity values were measured before (I_0) and after (I_{30}) the endonuclease cleavage of DNA probes. For each reaction set, the data were normalized to the initial fluorescence signal and the represented ratio describes the net of CpG sites remained un-cleaved (± S.D., n=80). The methylation reaction efficiency was calculated as a percent of methylated CpG sites comparing to positive (5mC+) and negative (5mC-) controls of methylation. On the bottom, the corresponding experiment in SDS-PAGE demonstrates the separation of DNA fragments following the endonuclease cleavage. b) Varying concentrations of *HPAII* DNMTase were incubated with unmethylated DNA probe and the resulted dose-response curve was fitted by non-linear regression of the Michaelis-Menten equation.

Further, we evaluated the steady-state and the kinetic properties of *HPAII* DNMTase, demonstrating the quantitative nature of the microfluidic platform. The steady-state Michaelis–Menten constant, K_m, was evaluated for each of the substrates, DNA and SAM. As expected of multi-substrate reactions, the remaining fluorescence signal (representing the methylation product, 5mC) exhibited statistical dependence on both substrate concentrations with a K_m values of 5.8 nM and 9.8 nM for DNA and SAM, respectively (**Figure 4**a and b). In order to evaluate the catalytic constant (K_{cat}), the initial velocity of methylation reaction was estimated through four independent experiments using various concentrations of the enzyme (**Figure 4**c). The initial rates were linear with enzyme concentration, and a K_{cat} of 0.04 sec^{-1} was determined from the slope of the linear regression (**Figure 4**d).

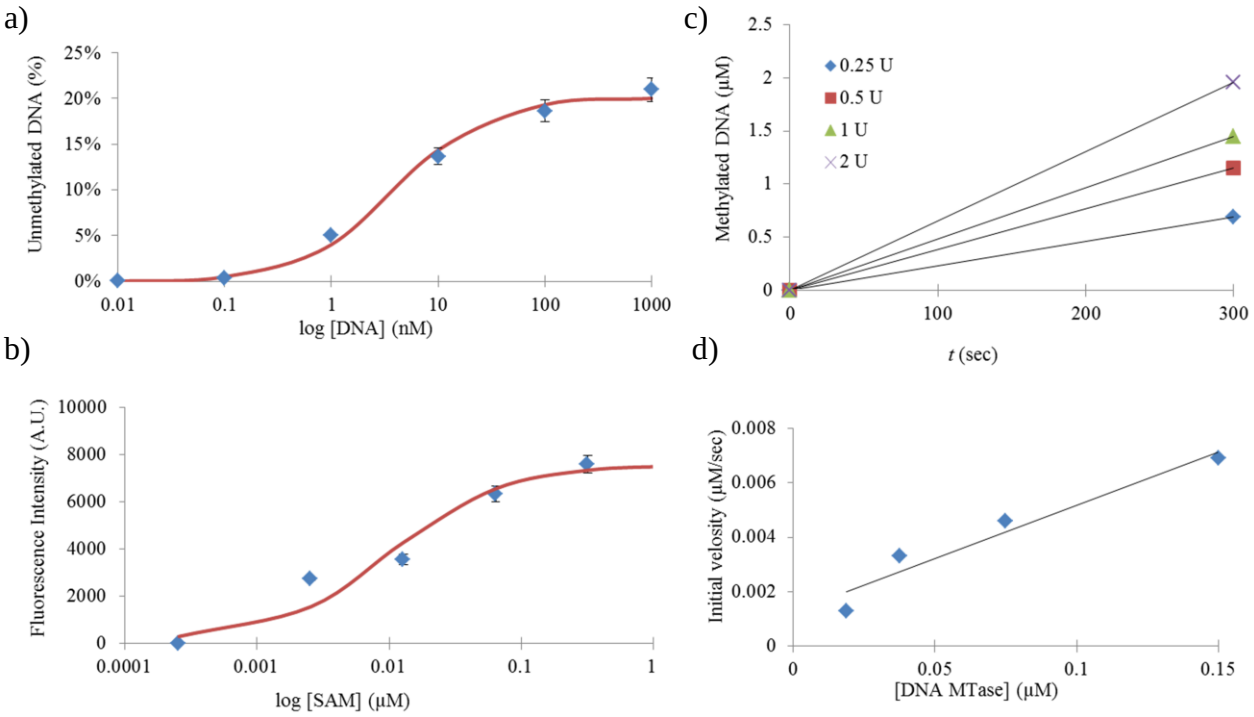

Figure 4. a,b) For K_m^{DNA} and K_m^{SAM} constants, the reactions were incubated in the presence of various concentrations of DNA or SAM and the data were fitted by non-linear regression to the Michaelis-Menten equation (± S. D., n=80). c) For K_{cat} determination, the initial velocity of the reaction was measured after 5 min for various DNMTase concentrations in four independent experiments. d) Initial rates were plotted against enzyme concentrations, and the K_{cat} was determined from the slope of the linear regression**.**

2.4 High-Throughput *On-chip* Inhibition Screen

In light of increasing interest in discovery of novel non-nucleoside inhibitors of DNMTases, we tested the compatibility of the microfluidic-based methylation assay with high throughput screening of chemical compound libraries for discovering non-nucleoside DNMTIs. As a proof of concept, we tested the ability of the microfluidic platform to screen inhibition of the bacterial *HPAII* DNMTase in high throughput. For this purpose, we created a microarray of chemical molecules emulating large-scale chemical compounds libraries used for inhibition screens. The array contained two known non-nucleoside inhibitors: a SAM-competitive quinoline-based compound SGI-1027 and RG108 that blocks the active site of DNMTase and renders the enzyme inactive. [29,30]. In addition, two molecules, ATP and nicotinamide (NAM), that do not have intrinsic inhibition potential were included in the array demonstrating the presence of chemical molecules whose impact on the methylation activity is not expected. The microarray was spotted on the glass slide

creating blocks of multiple repeats (n=64) that then was aligned to the microfluidic device while each spot is isolated within individual reaction chamber (**Figure 5**a). The microfluidic device can contain a maximal array of 16 row on 64 columns. The unspotted reaction chambers, that consisted the largest block, define regions of uninhibited methylation environment and were used as negative control of inhibition. The number of unspotted chambers emphasizes the potential of the microfluidic platform to contain large-scale chemical libraries. Moreover, larger capacities devices (64x64) with similar design and functionality are already available.[31]

On average, about 45% and 15% inhibition of *HPAII* DNMTase activity was observed for SGI-1027 and RG108, respectively, and no reduction was observed for any of the other molecules that served as negative controls (**Figure 5**b). The limited activity of RG108 was expected and could be further improved by using RG108-procainamide conjugates that showed much higher activity but were not commercially available at the time of the experiment.[32] These results demonstrate the ability of the microfluidic-based methylation assay to detect inhibition of DNMTase activity and emphasize the great potential of the microfluidic platform to screen thousands of chemical molecules for novel non-nucleoside DNMTIs.

2.5 Quantitative Measurements of the *On-chip* Inhibition

Following the high throughput inhibition screen, we quantified the half maximal inhibitory concentration (IC_{50}) of both DNMTIs using the same microfluidic platform. Values similar to what is described in the literature will demonstrate the quantitative nature of the inhibition assay within the microfluidic platform allowing proper quantitative assessment of the inhibition effect. For IC_{50} calculations, each candidate was examined separately using series of dose-response experiments. We used a dilution of 8 concentrations for each molecule and the number of each concentration repeats corresponds the number of reaction chambers within the single column (**Figure 5**c). According to expectations, the inhibition levels exhibited statistical dependence on inhibitor concentrations with IC_{50} values of 4.5μM for and 87.5nM for SGI-1027 and RG107, respectively (**Figures 5**d).

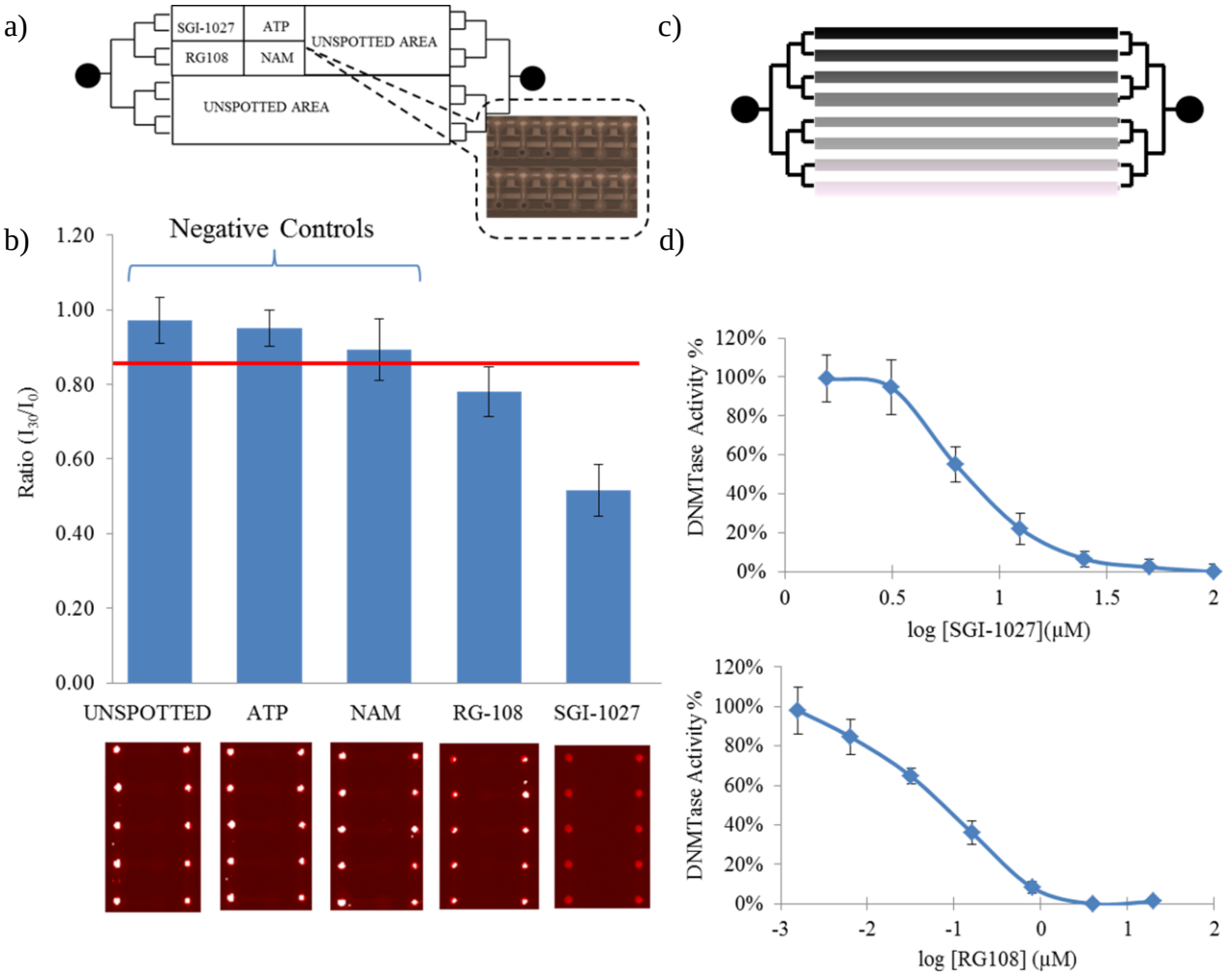

Figure 5. a) Illustration of the spotted and aligned DNMTI array that contains molecules without intrinsic inhibition potential (ATP and NAM) and two known non-nucleoside inhibitors (SGI-1027 and RG108). Each spotted block consists of 4 columns and 16 rows. b) Following the incubation of unmethylated DNA probe with DNMTase in presence of spotted DNMTIs, Cy5 intensity values were measured before (I_0) and after (I_{30}) of endonuclease cleavage. Each data set was normalized to the initial fluorescence signal within the corresponding block and the resulting ratio describes the net CpG sites remained un-cleaved (± S.D., n=64). The red line represents the inhibitory threshold determined as two standard deviations below the averaged 'unspotted' ratio. *On-chip* visualization of the corresponding remaining Cy5 signal is placed on the bottom of each column. c) Schematic representation of DNMTI dilution concentrations separated within isolated columns to prevent mixing. A dilution of 8 concentrations was used for each molecule in 128 repeats (as the number of reaction units within the pair of adjacent columns). d) Graphical representation of the concentration-dependent inhibition by SGI-1027 (top) and RG107 (bottom) used for IC_{50} calculations.

3. Discussion

In mammals, DNA methylation provides heritable, long-term chromatin regulation and aberrant methylation patterns have been associated with imprinting-related diseases, auto-immune, mental disorders and cancer.[7,33,34] The current epigenetic treatment is based on reactivation of tumor-suppressing genes by non-specific, cell-cycle dependent inhibition of DNMTase activity. The mode of action for such drugs is associated with global DNA demethylation leading to genomic

instability. Consequently, there is a continuous research in the field of non-nucleoside DNMTIs, which may reduce the adverse effects associated with current nucleoside-based epigenetic therapies. Another model of epigenetic therapy suggests that DNMTase substrate specificity, sequence targeting, and/or regulated enzymatic activity is disrupted in tumor cells due to aberrant protein-protein interactions with DNMTase-associated proteins or protein complexes in which DNMTases reside.[35] Therefore, identifying those interactions and characterizing their impact on DNA methylation may complete the picture of DNA methylation pattern establishment and maintenance and shed light on the nature of the methylation defect in tumor cells, and other deseases. In both cases there is a need in development of sensitive high-throughput platforms for screening larger and more diverse libraries of chemical/biological matter to discover additional candidates able in direct regulation of DNMTase activity.

We developed a simple, fluorometric, microfluidic-based assay of DNMTase activity that uses an approach of methylation-sensitive endonuclease digestion of DNA substrate probes. Coupling this assay to the microfluidic platform allows for simultaneous experimentation of thousands of methylation reactions on a single device within isolated chambers. The DNA probe immobilization through biotin concentrates the fluorescence signal and enhances the sensitivity, resulting in a wide dynamic range observed. Moreover, it reduces the amount of DNA substrate required, leading to significant cost reduction. We estimate that under a femto mole of DNA probes are immobilized to the surface of each reaction chamber.

We quantitatively reproduced the methylation activity of *HPAII* DNMTase by measuring the steady-state and the kinetic properties of the enzyme and observed approximately 97% methylation of all methylation sites available. The values measured were found in a close agreement with those previously published for *MSP1*, a known isochizomer (**Table 1**).[36] We then tested the ability of the microfluidic platform to screen direct inhibition of bacterial DNMTase in high throughput by coupling the methylation assay with an array of selected chemical compounds. We reproduced the inhibition potential of two known non-nucleoside DNMTIs, SGI-1027 and

RG108, from the spotted microarray while no inhibition was observed for any other of the spotted molecules that do not have intrinsic inhibition potential. These results show, as a proof of concept, the compatibility of the microfluidic-based methylation assay with high throughput qualitative screening of chemical compound libraries for novel non-nucleoside DNMTIs. Similar design and functionality microfluidic devices with larger capacities (64x64) allowing for screening thousands of molecules are already available and can be used to screen large-scale libraries of chemical compounds.[31] We followed the qualitative inhibition screen by calculating the IC_{50} of both DNMTIs and found all values in close similarity to the manufacturer declared data (**Table 2**). The microfluidic platform allows coupling the high-throughput screening of chemical libraries with quantitative assessment of inhibition potential. This two-step approach emphasizes a great potential of the microfluidics in performing a complete process of novel non-nucleoside DNMTIs identification and characterization *in-vitro* using a single platform.

We believe this platform can be further used for studying functional regulation of human DNMT family members by cellular proteins *in vitro.* In this relation, the microfluidic platform offers a great advantage of effective, high-throughput synthesis of large-scale protein libraries from an array of spotted DNA templates using cell-free transcription-translation system.[27,28] Following the expression, each of the thousands of proteins in the array will be simultaneously subjected to the *in-situ* DNMTase-induced methylation reaction within the isolated reaction units. The regulation potential of each protein on DNMT methylation activity will be characterized by comparing to reference reactions with no added proteins. Moreover, the microfluidic platform could be optimized to study other aspects of DNA methylation dynamics. For example, an oxidation-dependent active DNA demethylation has become a subject of intensive research in a last few years.[37–39] By replacing the cytosine with 5-hydroxymethylcytosine residue, this assay could be applied for studying the regulation of TET family proteins by endogenous protein factors.

In conclusion, we developed universal, sensitive, non-radioactive assay that can be used for a broad range of DNA methylation dynamic analysis *in-vitro*. Coupling this assay to a high-

throughput microfluidic platform may open new horizons for epigenetic research and even lead to novel therapies to reverse aberrant methylation patterns in tumor cells, and other diseases.

Table 1. The measured kinetic parameters of *HPAII* are comparable to the published parameters for its isochizomer *MSPI*. Simultaneously

	K_m^{DNA} (nM)	K_m^{SAM} (nM)	K_{cat} (sec^{-1})
HPAII	5.8	9.8	0.04
MSPI	4.4-7.69	12.7-16.32	0.056

Table 2. The measured IC_{50} of known DNMTIs are comparable with the literature.

	Methylation Assay	Manufacture Data
SGI-1027 (µM)	4.5	6-8
RG108 (nM)	87.5	115

Acknowledgements

This work was supported by the ERC-STG grant no. 309600.

References

1. R. Holliday and J. E. Pugh, *Science (New York, N.Y.)*, 1975, **187**, 226–232.
2. T. Rein, *Nucleic Acids Research*, 1998, **26**, 2255–2264.
3. Z. Siegfried and H. Cedar, *Current biology : CB*, 1997, **7**, R305–7.
4. A. D. Riggs, *Cytogenetics and cell genetics*, 1975, **14**, 9–25.
5. R. Bonasio, S. Tu, and D. Reinberg, *Science (New York, N.Y.)*, 2010, **330**, 612–6.
6. S. Feng, S. E. Jacobsen, and W. Reik, *Science (New York, N.Y.)*, 2010, **330**, 622–627.
7. A. P. Feinberg and B. Tycko, *Nature reviews. Cancer*, 2004, **4**, 143–53.
8. X. Yang, F. Lay, H. Han, and P. A. Jones, *Trends in pharmacological sciences*, 2010, **31**, 536–546.
9. J. K. Christman, *Oncogene*, 2002, **21**, 5483–5495.
10. V. Gorbunova, A. Seluanov, D. Mittelman, and J. H. Wilson, *Human molecular genetics*, 2004, **13**, 2979–2989.
11. C. Mund, B. Hackanson, C. Stresemann, M. Lübbert, and F. Lyko, *Cancer research*, 2005, **65**, 7086–7090.
12. F. Lyko and R. Brown, *Journal of the National Cancer Institute*, 2005, **97**, 1498–506.
13. T. K. Kelly, D. D. De Carvalho, and P. A. Jones, *Nature biotechnology*, 2010, **28**, 1069–1078.
14. P. Neuži, S. Giselbrecht, K. Länge, T. J. Huang, and A. Manz, *Nature Reviews Drug Discovery*, 2012, 11, 620–632.
15. E. K. Sackmann, A. L. Fulton, and D. J. Beebe, *Nature*, 2014, **507**, 181–9.
16. G. M. Whitesides, *Nature*, 2006, **442**, 368–373.

17. D. Mark, S. Haeberle, G. Roth, F. von Stetten, and R. Zengerle, *Chemical Society reviews*, 2010, **39**, 1153–1182.
18. T. Squires and S. Quake, *Reviews of Modern Physics*, 2005, 77, 977–1026.
19. M. Balaghi and C. Wagner, *Biochemical and biophysical research communications*, 1993, **193**, 1184–1190.
20. J. Soares, A. E. Pinto, C. V. Cunha, S. André, I. Barão, J. M. Sousa, and M. Cravo, *Cancer*, 1999, **85**, 112–118.
21. J. Singer-Sam, J. M. LeBon, R. L. Tanguay, and a D. Riggs, *Nucleic acids research*, 1990, **18**, 687.
22. M. Weber, J. J. Davies, D. Wittig, E. J. Oakeley, M. Haase, W. L. Lam, and D. Schübeler, *Nature genetics*, 2005, **37**, 853–862.
23. F. V. Jacinto, E. Ballestar, and M. Esteller, *BioTechniques*, 2008, **44**, 35, 37, 39 passim.
24. B. A. Flusberg, D. R. Webster, J. H. Lee, K. J. Travers, E. C. Olivares, T. A. Clark, J. Korlach, and S. W. Turner, *Nature methods*, 2010, **7**, 461–465.
25. V. J. Bailey, H. Easwaran, Y. Zhang, E. Griffiths, S. A. Belinsky, J. G. Herman, S. B. Baylin, H. E. Carraway, and T.-H. Wang, *Genome research*, 2009, **19**, 1455–1461.
26. L. Shen and R. A. Waterland, *Current opinion in clinical nutrition and metabolic care*, 2007, **10**, 576–581.
27. D. Gerber, S. J. Maerkl, and S. R. Quake, *Nature Methods*, 2009, **6**, 71–74.
28. Y. Glick, D. Avrahami, E. Michaely, and D. Gerber, *Journal of visualized experiments : JoVE*, 2012, e3849.
29. J. Datta, K. Ghoshal, W. A. Denny, S. A. Gamage, D. G. Brooke, P. Phiasivongsa, S. Redkar, and S. T. Jacob, *Cancer research*, 2009, **69**, 4277–4285.
30. B. Brueckner, R. Garcia Boy, P. Siedlecki, T. Musch, H. C. Kliem, P. Zielenkiewicz, S. Suhai, M. Wiessler, and F. Lyko, *Cancer research*, 2005, **65**, 6305–6311.
31. P. M. Fordyce, D. Gerber, D. Tran, J. Zheng, H. Li, J. L. DeRisi, and S. R. Quake, *Nature biotechnology*, 2010, **28**, 970–975.
32. L. Halby, C. Champion, C. Sénamaud-Beaufort, S. Ajjan, T. Drujon, A. Rajavelu, A. Ceccaldi, R. Jurkowska, O. Lequin, W. G. Nelson, A. Guy, A. Jeltsch, D. Guianvarc'h, C. Ferroud, and P. B. Arimondo, *Chembiochem : a European journal of chemical biology*, 2012, **13**, 157–65.
33. I. P. Pogribny and F. A. Beland, *Cellular and molecular life sciences : CMLS*, 2009, **66**, 2249–61.
34. C. B. Santos-Rebouças and M. M. G. Pimentel, *European journal of human genetics : EJHG*, 2007, **15**, 10–7.
35. K. D. Robertson, *Oncogene*, 2001, **20**, 3139–55.
36. S. K. Bhattacharya, *Journal of Biological Chemistry*, 1999, **274**, 14743–14749.
37. J. U. Guo, Y. Su, C. Zhong, G. Ming, and H. Song, *Cell*, 2011, **145**, 423–34.
38. M. Tahiliani, K. P. Koh, Y. Shen, W. A. Pastor, H. Bandukwala, Y. Brudno, S. Agarwal, L. M. Iyer, D. R. Liu, L. Aravind, and A. Rao, *Science (New York, N.Y.)*, 2009, **324**, 930–5.
39. Z. Gong and J.-K. Zhu, *Cell Research*, 2011, 1–3.